The performance of leaching experiments to assess the potential mobilization of trace elements during CO2 injection

The performance of leaching experiments to assess the potential mobilization of trace elements during CO_2 injection

Mark Wilkinson, Kit Carruthers, Alexander L. Thomas, R. Stuart Haszeldine

School of GeoSciences, Grant Institute, The King's Buildings, James Hutton Road, Edinburgh EH9 3FE, UK

Corresponding author: Mark Wilkinson, mark.wilkinson@ed.ac.uk

ABSTRACT

To control reservoir pressure during CO_2 injection for Carbon Capture and Storage, it may be necessary to produce native porewaters to the surface. These porewaters could contain potentially toxic metals mobilised from the reservoir rock by the injected CO_2, which would then be discharged into the ocean if offshore, or treated if onshore. To evaluate the risk, both chip and grain samples from a UK North Sea sandstone that is a candidate for CO_2 storage were exposed to CO_2-saturated water in 30 day leaching experiments, and the metal load of the porewaters was analysed. Only Pb and Zn were convincingly mobilised (median 30 vs 2 μg/L for Pb; 130 vs 25 μg/L for Zn), and these elements these have been previously reported to be more easily mobilised in experiments than during in-situ CO_2 injection. Hence, in this case, the risk of releasing toxic metals into the environment is assessed as small, and comparable to existing hydrocarbon operations. Results are significantly variable within a single sandstone reservoir, suggesting that experiments with multiple samples are required to make a realistic assessment of leaching potential. An assessment of other potential chemical data for assessing trace metal leaching suggested that only the comparatively lengthy leaching experiments generated useful data.

1. Introduction

Carbon capture and storage technology is being implimented at industrial scale in several locations worldwide. Finding sufficient secure storage is essential, and a limiting factor in the storage capacity of many sites will be the build-up of porewater pressure during injection (e.g. SCCS, 2011). One solution to control subsurface pressure, and hence to increase storage capacity, is to produce porewater from the reservoir to the surface (SCCS, 2011). This porewater could potentially contain some dissolved CO_2, although the return of CO_2 back to the surface will obviously be kept to an absolute minimum. Potentially toxic trace metals may have been mobilised from the reservoir rock into the porewater, which will require safe disposal. There are now multiple papers focused on CO_2 – water - rock interactions with respect to underground CO_2 storage, and the potential environmental impacts. The published literature encompasses modelling, laboratory, and field experiments, with environmental impacts of CO_2 leakage on groundwater quality considered in more recent publications (e.g. Kirsch et al. 2014; Lu et al. 2014; Zheng and Spycher, 2018). Field studies have also

focussed on the environmental impacts of CO_2 release into underground supplies of potable water as an aid to understanding in-situ reactions (e.g. Cahill et al. 2013; Trautz et al. 2013), as opposed to often far-from-equilibrium laboratory experiments.

This paper deals with the Captain Sandstone Member of the Moray Firth of Scotland (Fig. 1) which has been extensively studied previously as a site for the engineered storage of CO_2. A report commissioned by the UK government identified a portion of the sandstone, known as the Captain X site, as one of the 5 most promising CO_2 storage sites on the UK Continental Shelf (UKCS; Pale Blue Dot Energy, 2016). The storage capacity of the site was estimated as 60 Mt CO_2 (Pale Blue Dot Energy, 2016). Earlier work on the same sandstone member concluded that the capacity of the entire sandstone (as opposed to the geographically-restricted Captain X site) varied from 358 to 1668 Mt CO_2, depending on assumptions about the geometry, geomechanical properties of the reservoir and the nature of the boundaries of the sandstone (SCCS, 2011). A key finding was that, for maximum storage capacity, large volumes of porewater from the reservoir might have to be produced to the surface, and disposed of, most probably by discharging into the sea ('over-boarding'). To reduce the uncertainty in storage capacity, and hence the risk of investment in a CCS project in the Captain Sandstone Member, it would likely be necessary to plan for the production of porewaters to the surface, even though it may not be needed. The environmental risks of such a strategy must hence be evaluated, even though every effort would be made to avoid the production of CO_2-laden waters back to the surface, as this would defeat the purpose of injection.

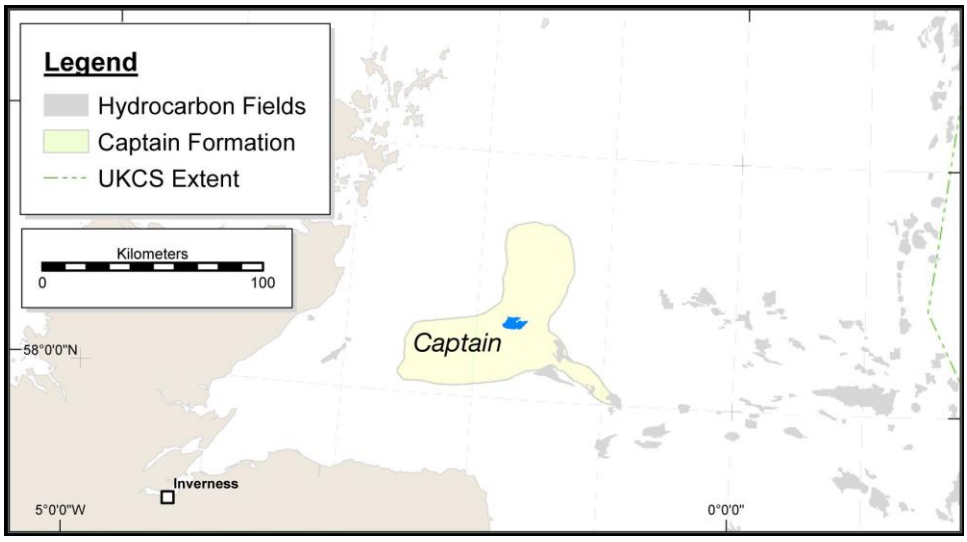

Fig. 1 – Location map showing the extent of the Captain Sandstone Member (yellow), and the Captain hydrocarbon field (blue).

In this study, experimental work under controlled laboratory conditions that are representative of reservoir temperatures has been carried out to determine how reservoir rocks from the Captain Sandstone Member react when CO_2 is introduced. Our results are compared to a database of bi-annually reported metal concentrations (As, Cd, Cr, Cu, Pb, Hg, Ni and Zn) in produced waters associated with hydrocarbon production from the Captain Sandstone Member. These monitoring

data were compiled since 2006 as required for some permits for hydrocarbon production in the Environmental and Emissions Monitoring System (EEMS, https://www.gov.uk/oiland-gas-eems-database; obtained January 2015). This allows for the comparison of the experimental results to analyses of porewaters routinely discharged into the North Sea during oil industry operations utilising the same reservoir sandstone. It is assumed here that the EEMS analyses are representative of the in-situ porewaters in the subsurface, henceforth called the native porewaters.

The Captain Sandstone Member is a Lower Cretaceous mass-flow sandstone-dominated unit of up to 200 m thickness (Pinnock et al., 2003) covering c. 4000 km^2 (from maps in SCCS, 2011). The sandstone forms the reservoir for several commercial hydrocarbon fields, including the Captain Field. The porewaters within the Captain Sandstone Member are below seawater salinity (12 – 25,000 ppm TDS; Pinnock et al., 2003), and have been routinely discharged into the North Sea during hydrocarbon production. The Captain Sandstone Member in the Blake Field, the source of the experimental samples, is reported to be at 56°C and c. 330 bars pressure (Melvin et al., 2008), representing a significant overpressure.

2 Materials & methods

The study rock is hydrocarbon reservoir core from the Blake Field borehole 13/24a-4 (Table 1), drilled in December 1997 to January 1998. The sandstone samples were collected from the UK national collection stored by the British Geological Survey. Both samples were characterised using thin-sections impregnated with a blue-dyed resin examined with a petrographic microscope. Porosity and mineral abundance were determined by point-counting 200 points per thin-section in a grid pattern. Phases recognized during the thin section analysis but not recorded in the point counting have been recorded as present in quantities < 1%. Sample SA7 was oil stained and smelled of oil, while sample SA10 had no obvious oil contamination. Grain size was determined using a calibrated graticule on the microscope eyepiece.

2.1 Leaching experiments and water analysis

Rock samples were introduced to the reaction vessels as either chips of approximately 1 cm diameter, or as disaggregated grains. Sample preparation used a geological hammer and mortar and pestle; disaggregation required minimal force due to the low degree of consolidation of the material. Samples were added at the weights given in Table 1, to 250 mL of brine of 13,500 mg / L salinity made using Fisherbrand 'SLR' grade sodium chloride solid reagent and 11 mΩ /cm high purity water from a Milli-Q water system. The NaCl has < 0.5 ppm of relevant specified impurities (Cu, Pb and Zn) which equates to less than 10 ppb in solution, significantly below the limit of analytical detection. It is assumed that the elements of interest that are not in the manufacturer's specification are present in equally low concentrations. The reaction vessels were held at atmospheric pressure and a target temperature of 56 °C, with measured fluctuation between c. 55 and 58 °C and extremes of 50 – 68 °C, for 30 days. Blank samples, i.e. with no rock, were run both with (CAP_F1) and without (CAP_B1) CO_2. Although the partial pressure of oxygen within the vessels was presumably somewhat lower

than the surrounding atmosphere, the conditions were still oxidising. No attempt was made to reproduce reducing conditions as might be anticipated in the subsurface.

Table 1. Batch experiment configurations. CO_2 flow refers to the presence (Y) or absence (N) of bubbled CO_2 in the experiment.

Sample Name	Sample depth (DD m)	Sample type	Sample Weight (g)	CO_2 Flow
CAP_F1		blank	0	Y
CAP_SA7_F2	1620	chip	3.36	Y
CAP_SA7_F3	1620	grain	2.75	Y
CAP_SA10_F4	1656	chip	3.36	Y
CAP_SA10_F5	1656	grain	2.64	Y
CAP_B1		blank	0	N
CAP_SA7_B2	1620	chip	3.17	N
CAP_SA7_B3	1620	grain	2.75	N
CAP_SA10_B4	1656	chip	3.18	N
CAP_SA10_B5	1656	grain	2.85	N

The batch reaction vessels were Quickfit™ 250 mL round bottomed, three necked borosilicate flasks with Liebig condensers. Prior to set up, all glassware and sampling vessels were soaked in a 10% nitric acid bath for at least 12 hours, rinsed with distilled and deionised water (11 mΩ / cm), and air dried. Glassware was then wrapped in aluminium foil and dried at 450° C for four hours to destroy any residual organic material, and left wrapped in the foil until the experiment was set up. Dry CO_2 gas was fed to each flask where appropriate from a BOC vapour withdrawal CO_2 bottle with attached 2 bar regulator, to glass injection tubes. CO_2 flow was regulated using Hoffman tubing clamps to maintain a pressure of 1.4 bar to bubble CO_2 into the batch fluids. Fluid samples were drawn from the batch flasks using a pipette and passed through a 0.22 µm filter into PTFE sample bottles, acidified to 2% v / v with analytical grade 69 % HNO_3 and refrigerated prior to analysis. Results were obtained for 3 categories of experiment: blanks (no rock, with or without CO_2); rock plus added CO_2, henceforth referred to as +CO_2 experiments; and controls i.e. rock with no added CO_2. Solution composition during the experiments was modelled using PHREEQC v3.3.3 using mineralogy from X-ray diffraction (see below) and the database Phreeqc.dat. The fluid was modelled as either saturated with air, or with CO_2 as appropriate.

Batch fluid samples were analysed by ICP-MS for major and trace elements using an Agilent 7500ce with octopole reaction system, employing an RF forward power of 1540 W, reflected power of 1 W, argon gas flows of 0.82 L/min and 0.2 L/min for carrier and makeup flows, respectively, and nickel skimmer and sample cones, with a Micro mist nebuliser and peristaltic pump providing a solution uptake rate of approximately 1.2 mL/min. The instrument was operated in spectrum multi-tune acquisition mode and three replicate runs per sample were employed. Calibration was with Merck VI multi-element ICP standard with the exception of Hg, which was calibrated with a BDH 'SpectrosoL' ICP-MS standard, and Cs, P, Sb, Si, Sn, Th, Ti and Zr which were calibrated with SPEX Certiprep R or Fisherbrand ICP-MS standards. All standards were made up with the same NaCl concentration as the samples to be analysed.

Zero values in the experimental data refer to concentrations less than the analytical limit of detection (LOD; Table 2). As calculated mean concentrations are dependent on the LOD, median values are quoted which are independent of the LOD, except in the case that the median value is the LOD e.g. for Cd. The LOD was calculated using analyses of 10 blank aliquots of sample matrix and 2% HNO_3 solutions. The instrumental LOD was calculated as 3σ of the blanks' ICP-MS counts per second divided by the slope of calibration line (Vandecasteele and Block, 1993). Concentrations of elements in the blank flasks (which had no rock samples) are assumed to be representative of any background concentrations of elements present in the fluid samples. As the majority of these were below detection limits no correction was made the experimental data for background levels of contamination. Detection limits are not published for the EEMS dataset.

The mass of element mobilised during the leaching experiments was calculated using the measured concentrations multiplied by the volumes of fluid extracted from the flasks for each measurement. For concentrations below the limit of detection, a value equal to the limit of detection was assumed, to produce a 'worst-case' maximum value for the quantity of element mobilised.

Table 2 – Detection limits (LoD) for by ICP-MS trace elements

Element	LoD μg / L	Predicted no-effect concentrations* μg / L	Seawater concentration μg / L
As	0.26	0.6 + Cb	0.75 – 4.0; Cutter et al. (2001)
Cd	0.005	0.2 + Cb	0.00 – 0.11; Middag et al. (2018)
Cr	0.08	0.6 + Cb	0.10 – 0.21; Jeandel and Minster (1987)
Cu	2.9	2.6	0.00 – 0.32; Boiteau et al. (2016)
Hg	0.02	0.05 + Cb	0.00 – 0.50; Bowman et al. (2015)
Ni	0.04	8.6 + Cb	0.12 – 0.47; Schlitzer et al. (2018)
Pb	0.13	1.3	0.00 – 0.01; Schlitzer et al. (2018)
Zn	1.8	3.4 + Cb	0.00 – 0.52; Wyatt et al. (2014)

* Cb = background concentration; OSPAR Commission (2014)

pH was measured by drawing 5 mL of fluid from the batch flasks using pipettor, transferring to a, rinsed, acid cleaned vial, cooling in air to approx. 26 - 27°C and analysing with a Hanna HI9125 pH meter with attached glass VWR ceramic junction pH electrode, calibrated with Hanna HI7007 (pH 7.01) and HI7004 (pH 4.01) NIST traceable buffer solutions, accurate to ± 0.01 pH. Due to degassing of CO_2 during cooling of the samples, the pH data are not regarded as being very reliable.

Alkalinity was measured as bicarbonate (mg/L) using a Palintest Photometer 7100, accurate to ± 5 mg/L and with a 2σ repeat measuring precision of 5.7 %. Measurements were taken by crushing a Palintest alkophot 'M' reagent tablet in 9 mL of sample, immediately after removal from the batch flask. The photometer was calibrated with a blank of 9 mL of NaCl solution of the same concentration as the synthetic batch fluids. For the majority of the pH values obtained for the experiment (4.8 - 8.5 for non-blank experiments), bicarbonate is the dominant carbonate species and therefore a reasonable proxy for total alkalinity.

2.2 Bulk rock geochemistry

Bulk chemical analysis of the sandstone samples was carried out by complete dissolution of sample SA7 (insufficient sample SA10 remained) by microwave acid digestion using the following procedure. Four mL of concentrated HF, 3 mL concentrated HNO_3 and 2 mL 30 % HCl were added. In a CEM Mars Xpress system, a set of 24 samples including procedural blanks and 2 soil standard reference materials (NIST SRM2710a and SRM2711a) were digested in closed vessels at 200 °C for at least 30 minutes. The digested samples were evaporated to near dryness in the microwave system, using a MicroVap accessory. Samples were then taken up in the microwave in 10.5 ± 0.3 mL 2% HNO_3, at 180 °C. The resulting solution was analysed by ICP-MS as above. Uncertainties were calculated from three repeated analyses of the sample. Due to the microwave digestion method employed, Si volatises as hexafluorosilicic acid and therefore Si was not determined.

2.3 Sequential extraction procedure

A sequential extraction procedure (SEP) was performed on sample SA7 using a modified version of the method presented by Wigley et al. (2013) to include an additional step to target sulphide mineral phases, which replaced the hydrochloric acid step. Sample and reagent masses and volumes were taken from Tessier et al. (1979). 10 g each of sample were crushed with a mechanical jaw crusher and the resulting chips ground to a powder with a tungsten-carbide mill. Samples were homogenised and 1,000 ± 2 mg transferred to 50 mL centrifuge tubes. Reagents were added to the centrifuge tubes in the steps listed below.

1. Water: 8 mL 18.2 MΩ de-ionized (D.I.) water with continuous agitation for 2 hours.

2. Exchangeable fraction: 8 mL 1M sodium acetate solution at pH 8.2, with continuous agitation for 3 hours.

3. Carbonates: 8 mL 1 M sodium acetate adjusted to pH 5 with acetic acid, with continuous agitation for 7 hours, repeated 3 times with fresh reagent.

4. Oxides: 8 mL 0.1 M ammonium oxalate buffer adjusted to pH 3 with oxalic acid. Occasional agitation for 54 hours, repeated 3 times with fresh reagent.

5. Sulphides: 3 mL 0.02M nitric acid + 5 mL of 30% hydrogen peroxide adjusted to pH 2 with concentrated HNO_3, heated to 85 °C in a water bath for 2 hours with occasional agitation.

Added 3 mL hydrogen peroxide, adjusted to pH 2 with nitric acid, and heated again for 3 hrs. After cooling to approximately room temperature, 5 mL of 3.2 M ammonium acetate in 20% (v/v) nitric acid was added and the whole mixture diluted to 20 mL with D.I. water before continuous agitation for 30 mins.

6. Bulk digestion / silicates: Microwave digestion as above.

All continuous agitation was carried out by means of a rotating 'end-over-end' shaker connected to a voltage controller to adjust rotating speed. With the exception of Step 5, all SEP steps were carried out at a room temperature of c. 21 ° C. After each extraction period the samples and supernatants were centrifuged at 12,000 rpm for 20 minutes, and the supernatants removed from the centrifuge tubes by carefully pouring out into an acid cleaned vial. This centrifugal speed was higher than the

Wigley et al. (2013) method as their speed was not sufficiently high to ensure that any clays in suspension in the supernatant 'plate out' during centrifugation. Although the clays plated out at the higher centrifugal speed used in this work, nonetheless when the supernatants were removed, some of the finest solid material was re-suspended and transferred into the sub-sampling vial. This was most pronounced after the first step using deionised water and became less apparent throughout the remainder of the steps. Each supernatant was filtered through a 0.22 μm filter into the final sampling vessel. Each sample was acidified with 2% nitric acid and refrigerated for preservation until analysis.

Bulk mineral analysis was carried out using a Bruker D8-Advance X-ray Diffractometer, employing a 2-theta (2θ) configuration, with X-rays generated by a Cu-anode X-ray tube operating at 40 kV, and a tube current of 40 mA. Diffracted X-rays were detected using a Sol-X energy dispersive detector, scanning from 2° to 60° 2θ at a scan rate of 0.01°/second and the resultant diffractograms compared with the 2008 issue of the International Centre for Diffraction Data (ICDD) diffractogram database library using the EVA analysis package. The uncertainty in the analyses is calculated by the software. The detection limit for crystalline phases is approximately 1 wt %, with values of less this indicative of probable presence only.

3. Results

Table 3 summarises the petrography of the samples. The samples were only poorly consolidated, with very few occurrences of brittle deformation of framework grains. There was visible dissolution and alteration to kaolinite of some feldspars and minor chloritization of a lithic fragment. Thin green rims that could not be identified optically were observed on some grain surfaces in SA7. No cement was observed in SA10. A minority of grains are replaced by microcrystalline calcite. Both samples are sub-arkoses according to the classification of Folk (1974).

Table 3 – Sample petrography

	SA7 point count	SA7 XRD / wt %	SA10 point count	SA10 XRD/ wt %
Max grain size	1.2 mm		1.8 mm	
Min grain size	0.05 mm		0.006 mm	
Grain size	fine-medium sand		medium sand	
Sorting	moderate		moderate	
Roundness	angular to well rounded		sub-angular to well rounded	
Porosity	30 %		30	
Quartz	84	81 ± 1	82	88 ± 1
Feldspars	12	9 ± 1	16	5 ± 1
Biotite	<1		<1	
Muscovite / illite	1	3.3 ± 0.5	2	2.1 ± 0.5
Calcite	<1	1.6 ± 1.4	<1	0.4 ± 0.1
Kaolinite	<1	2.8 ± 0.6		0.9 ± 0.2
Chlorite		0.3 ± 0.3		3 ± 0.5
Glauconite	2		<1	

Opaque	1		<1	
Oxides/Hydroxides	<1		<1	
Zircon	<1			
Corundum	<1			0.7 ± 0.1
Anatase				1.0 ± 0.1
Lithic fragments			<1	
Halite		2.2 ± 0.1		

231

232 Porewater composition from the batch experiments are in Tables 4A and B. Figure 2 shows trace
233 metal concentration for the EEMS database and the batch reaction experiments for both the
234 controls and the CO_2 - experiments. Note that a substantial proportion of the experimental analyses
235 are below the limit of detection (BDL; Fig. 2), and are shown as '0' in Tables 4A and B. Analyses
236 below detection limits are not plotted on Fig. 2 but the numbers of such data are shown. Note that
237 approximately one half of the analyses are below detection limits (0 – 90 % for an individual
238 element; overall mean 57 ± 8 %). For most of the trace elements, the blank concentrations are
239 significantly lower than the experimental concentrations. However, for Hg, the blank concentrations
240 are comparable in magnitude to the experimental concentrations. For this reason, the Hg data in Fig.
241 2 are blank-corrected, i.e. the average blank analysis has been subtracted from the experimental
242 analysis for the same day for which samples were collected.

243

244 The range of trace element concentrations for the experiments are similar to those of the EEMS data
245 for As (median BDL [0.26 μg/L] with CO_2; 2.4 μg/L without CO_2; EEMS 1.0 μg/L), Cr (median 0.5 μg/L
246 with CO_2; BDL [0.08 μg/L] without CO_2; EEMS 0.7 μg/L), Hg (blank-corrected; median BDL [0.02 μg/L]
247 with CO_2; BDL without CO_2; EEMS 0.08 μg/L) and Ni (median 7.5 μg/L with CO_2; 1.7 μg/L without CO_2;
248 EEMS 3.0 μg/L). Element concentrations in the leaching experiments are substantially higher than
249 the EEMS data for Cu (median 100 μg/L with CO_2; 90 μg/L without CO_2; EEMS 0.8 μg/L), Pb (median
250 30 μg/L with CO_2; 2 μg/L without CO_2; EEMS 0.5 μg/L) and Zn (median 130 μg/L with CO_2; 25 μg/L
251 without CO_2; EEMS 9 μg/L). The experimental data for Cd appears to be higher (Fig. 2; median value
252 with CO_2 is BDL [0.005 μg/L]; without CO_2 is BDL; EEMS 0.05 μg/L) but 21 out of 32 analyses were
253 below detection limit in the +CO_2 experiments, so that overall the experimental data and the EEMS
254 data are comparable, or the +CO_2 experimental data may in fact be lower. A more quantitative
255 analysis is not possible given that the values of the analyses below detection limit are not known.
256 For Cu, the median of experiments is 90 - 100 μg/L, much higher than 0.8 μg/L for the EEMS data.
257 However for Cu both experiments with and without CO_2 have similar median values (90 versus 100
258 μg / L respectively). Hence, the only elements for which the CO_2 appears to have significantly
259 increased the trace element concentrations are Pb and Zn.

260

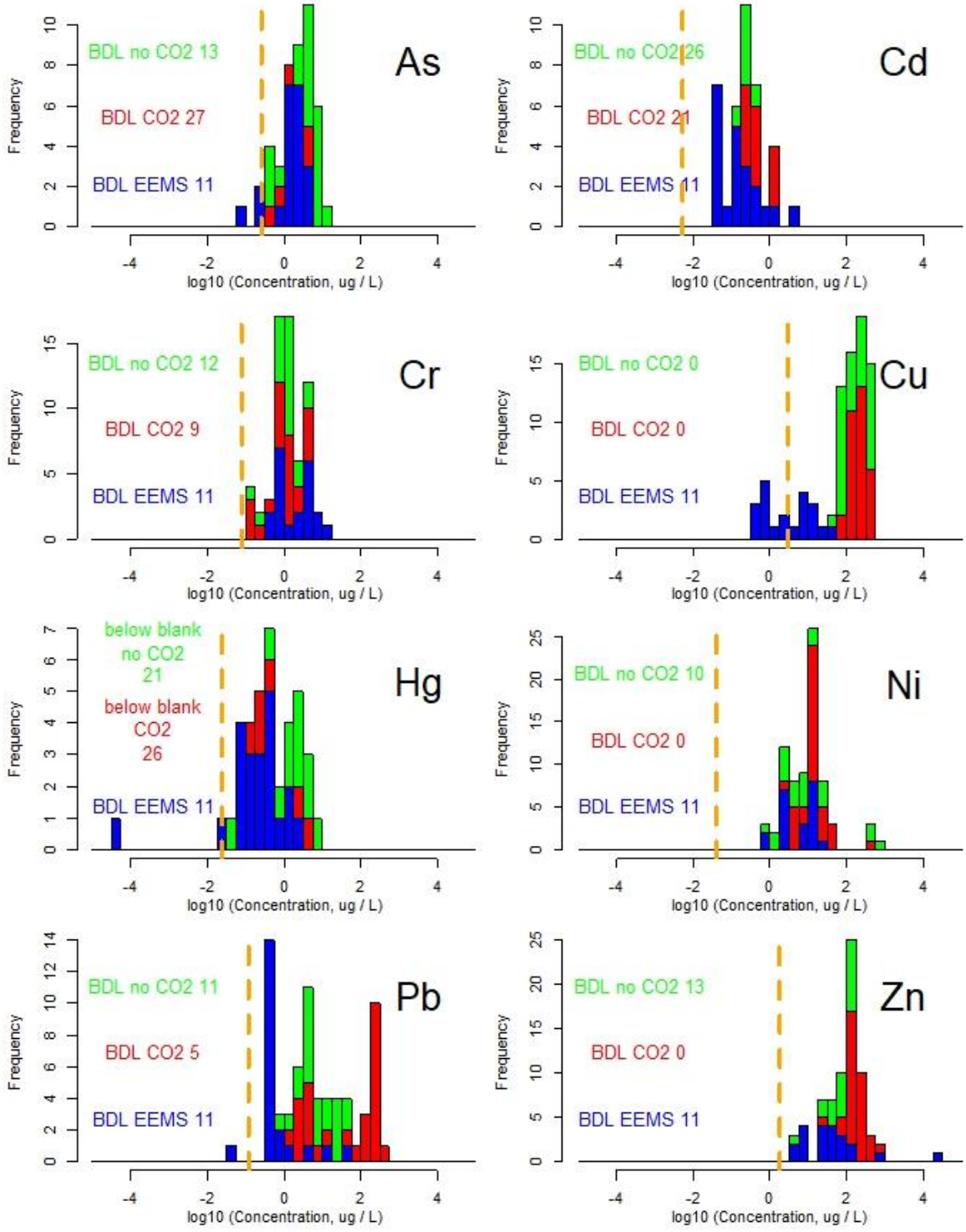

261

262 Fig 2 – Comparison of trace elemental concentrations from lab experiments and porewater from the
263 Captain Sandstone Member (EEMS database). The data that fall below the limit of detection (the
264 orange dotted line) are not plotted; the numbers of analyses that fall below this are given as below
265 detection limit (BDL). Green is experimental data with no added CO_2, red is experimental data with
266 added CO_2, blue is the EEMS dataset.

A time sequence of calculated trace element mass per g rock is shown in Fig. 3. Concentrations of arsenic are higher in the $-CO_2$ flasks than in those with added CO_2. In the majority of the experiments, the leached metal concentrations appear to have stabilised by the end of the experiments, i.e. to have reached an approximately constant value, or to be decreasing. The water-extractable metal loads determined on sample SA7 (shown as horizontal lines on Fig. 3) are not generally close to the leached loads for the same sample, with the possible exceptions of As, Hg for the $+CO_2$ experiments and Ni for the $-CO_2$ experiments.

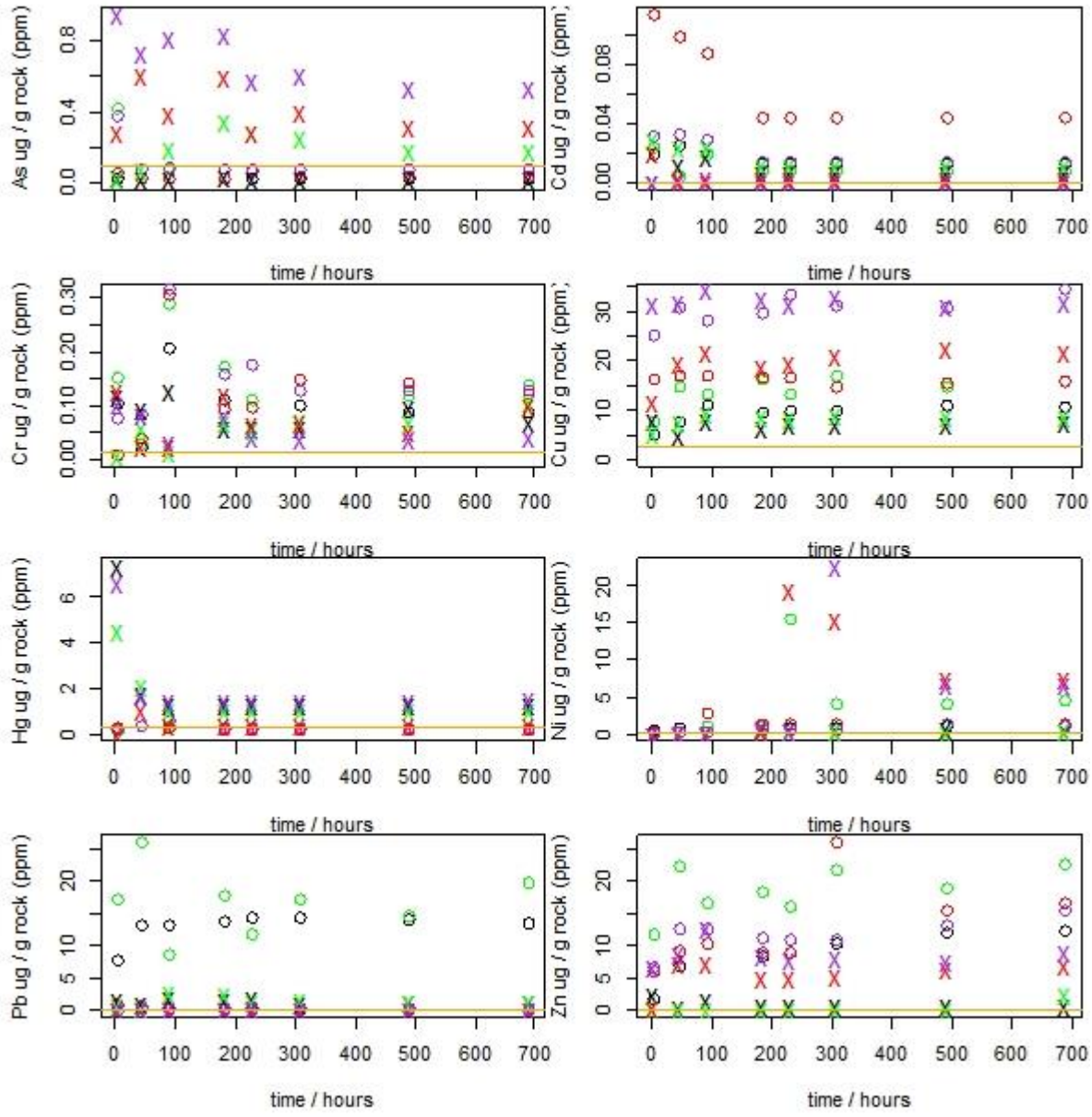

Fig. 3 – Calculated quantities of trace elements released from rock leaching experiments, through time, see methods section for details. Crosses are controls (no added CO_2), circles are with CO_2. Each colour represents a single experimental run. The horizontal orange lines are the concentrations from the water stage of the selective extraction procedure for sample SA7.

pH of the solutions varied from 3.9 - 5.4 for the blank flasks with added CO_2; 4.7 – 8.3 for blanks without added CO_2; 4.8 - 8.4 for flasks with rock sample and added CO_2; and 5.2 to 8.5 for flasks with no rock and added CO_2 (Tables 4A and B). Alkalinity values for the two blank flasks show a relatively small effect from the addition of CO_2, with values approximately constant through the duration of the experiment at 25 - 65 mg / L (blank +CO_2) and 20 - 70 mg / L (blank, -CO_2). Alkalinity values for sample SA7 without the addition of CO_2 are only slightly higher than the blanks at a range of 45 - 95 mg / L, while SA10 values without the addition of CO_2 increase from 80 mg/L to 165 mg/L. The addition of CO_2, however, increases alkalinity concentrations for both samples SA7 and SA10, with SA7 values increasing from 105 mg / L to 290 mg / L, and SA10 increasing from 135 mg / L to 500 mg / L (Tables 4A and B). The DIC of the solution during the experiments was modelled using PHREEQC as 0.024 mol / L assuming no reactants other than CO_2 and water, and as 0.036 mol / L with calcite present.

Bulk analysis of sample SA7 (Table 5) showed that of the 8 trace metals of interest, concentrations are generally < 10 ppm, with Cr and Zn being the (slight) exceptions. Cadmium concentrations are very low at 0.029 ppm. Results of the selective extraction procedure are in Table 6 and the water extraction stage is in Table 5 for the 8 trace metals. The mean proportion of the total elements leached in the experiments is very variable (Table 5), from a small fraction of the total in the bulk rock analysis (< 1 %; Cd, Cr) to greater than 50 % (Pb, Cu, Zn). As, Ni and Hg are intermediate.

299

300 Table 5: Bulk analysis of sample SA7 by ICP-OES unless indicated, and trace metals leached during
301 experiments and the water stage of the selective extraction procedure (SEP).

Element	Whole rock concentration μg/g	2σ (n = 3)	Element leached μg/g rock			
			range	mean –CO2	mean +CO2	Water stage of the SEP
Al	20,000	2,000				
As	4.3	0.7	0.02 – 1	0.32	0.07	0.1 ± 0.008
Ba	640	60				
Ca	5600	800				
Cd (ICP-MS)	160	0.001	0.0004 – 0.1	0.007	0.03	0.0008 ± 1e-5
Cr	24	3	0.006 – 0.3	0.067	0.13	0.013 ± 0.001
Cu	7.8	0.8	5 - 35	17	17	2.5 ± 0.1
Fe	5400	700				
Hg (ICP-MS)	5.9	1.2	0.1 - 130	1.5	0.27	0.3 ± 0.003
K	14100	800				
Li	14	2				
Mg	940	80				
Mn	54	7				
Na	6200	500				
Ni	5.9	0.7	0.003 – 23	2.9	1.7	0.25 ± 0.003
Pb	6.6	0.9	0.01 - 26	0.8	7.6	0.008 ± 0.0009
Ti	1500	200				
U	7.5	0.7				
Zn	16	2	0.2 - 26	3.9	13	0.11 ± 0.002

302

303 Results of X-ray diffraction (XRD) analysis of the unreacted rock samples (SA7 and SA10) are given in
304 Table 3, as weight %. Values of less than 1 % are indicative only of probable presence of a mineral in
305 the sample. Fe-oxides were not detected, neither were they positively identified in thin-section
306 using a petrographic microscope. However, thin green rims that could not be identified optically
307 were present on some grain surfaces in SA7, and these could include Fe-oxides. Geochemical
308 evidence (see below) suggests that Fe-oxides are present, presumably in concentrations below
309 detection limit for XRD.

310

311 Table 6: Results of the selective extraction procedure, units μg/g.

Element	Extraction stage						
	Water	Exchangeable	Carbonate	Oxide	Sulphide	Silicate	Bulk
Al	0	0	0.350	0	0	0	0
As	1.192	0	0	0.434	0	0	0

Ba	0	0.035	0	0.238	0.045	0	0
Ca	0	35.167	6.183	0	0	130.675	130.675
Cd	0.041	0.028	0	0	0	0.175	0.175
Cr	0.462	0.074	0	0	0	2.900	2.900
Cu	0.351	3.104	11.741	0	2.704	1.725	1.725
Fe	14.985	0	16.477	0.071	1.180	0	0
Hg	0	0	0.010	0.015	0.038		
K	0	45.850			0	0	0
Li	0.416	0	0	0	0	4.925	4.925
Mg	0.638	0.501	1.407	0	0.352	87.300	87.300
Mn	0	0.056	0.062	0	0	0	0
Na	83.075					568.475	568.475
Ni	0	1.137	0.809	1.381	2.109	0	0
Pb	0.174	0.103	0.039	0.012	0.040	0	0
Ti	0.280	0	0	0.011	0	0	0
U	0.028	0	0.000	0	0	0	0
Zn	1.283	3.369	0.547	0.158	2.475	10.075	10.075
n =	6	6	18	18	6	4	4

4. Discussion

The only metal with a strong decrease in concentration in the presence of CO_2 was arsenic (Fig. 3; median BDL [0.26 μg/L] with CO_2; 2.4 μg/L without CO_2). A relationship between Fe and As is demonstrated by Fig. 4, where As concentrations are only above c. 1 μg/L in solutions with low (< 100 μg/L) Fe. As arsenic (V) absorption onto Fe-oxides increases strongly with decreasing pH (e.g. Hsia et al., 1994), a simple pH control can be proposed. Any Fe-oxides could be an original component of the rock (perhaps the green rims on some grains in sample SA7); or formed by the oxidation of pyrite during the experiments; or during the storage of the core in the approximately 15 years between drilling and sampling. The latter is feasible, as pyrite is prone to reaction to oxy-hydroxides even in museum collections. The general decrease in As concentration during the experiments (e.g. c. 9 – 4 μg/L in experiment CAP_SA10_B5) could be interpreted as the progressive reaction from pyrite to Fe-oxides, increasing the surface area available for adsorption, or that adsorption is a slow reaction on the time scale of the experiments. Note that, although no sulphide minerals were detected by XRD analysis, the sulphide stage of the selective extraction procedure did generate metal concentrations above analytical detection limits that were dominated by iron, as might be expected if pyrite were present. The measured 260 μg / g of Fe liberated by the sulphide stage of the selective extraction procedure (Table 6) equates to c. 0.05 % pyrite, comparable to the 0.03 % of Allen et al. (2020, their Fig. 6) using QUEMSCAN analysis of a thin section of the Captain Sandstone, well below the detection limit for XRD. At least some of the remainder of the whole-rock Fe could be present as Fe-oxide coatings to detrital grains, however chlorite has a significant Fe content and is probably present in both rock samples (the 0.3% in SA7 is only an indicator of possible presence). Given the low abundance of chlorite (0.3 – 3 wt %), then separation for chemical analysis is considered to be impractical.

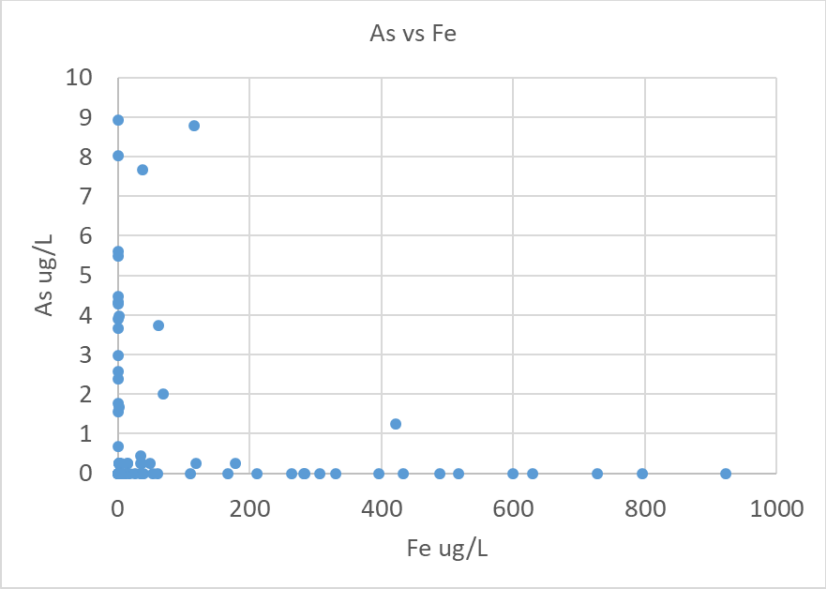

Fig. 4 – Arsenic concentrations are only above c. 1 μg/L in solutions with low (< 100 μg/L) Fe.

4.1 Comparison of experimental and natural water chemistry

A strong increase in the concentration of dissolved metals has been noted in previous studies of the effects of CO_2 in sandstones, and has been attributed to the dissolution of carbonates (e.g. Kjöller et al. 2011; Rosenbauer et al. 2005; Shiraki and Dunn 2000; Varadharajan et al. 2013), or desorption mechanisms (e.g. Cahill et al. 2013; Mickler et al. 2013; Varadharajan et al. 2013; Weibel et al., 2014). Slower releases of elements, e.g. Fe, K and Al are then attributed to silicate or oxide dissolution by these authors. For the experiments reported here, a strong case can only be made for Pb and Zn mobilisation by the added CO_2, in that for these elements the median experimental concentrations substantially exceed the EEMS data (Pb median 30 μg/L with CO_2; EEMS 0.5 μg/L; Zn median 130 μg/L with CO_2; EEMS 9 μg/L), and the element concentrations in the CO_2 experiments exceed those of the controls (Pb 2 μg/L without CO_2; Zn 25 μg/L without CO_2).

There is a strong 1:1 correlation between (Ca + Mg) and total alkalinity for both control and CO_2 flasks, and Ba, Ca, Fe, Mg, Mn, and Sr exhibit, in virtually all cases, enhanced concentrations with the addition of CO_2 (Table 4A). This suggests that these elements are derived by the dissolution of calcite, as the only carbonate phase detected by XRD analysis (Table 3), driven by pH changes of approximately -1 pH unit. Note that for two of the leaching experiments with added CO_2, the calculated quantity of Ca released per g of rock exceeds that in the bulk analysis (Fig. 5), interpreted to be a product of the uneven distribution of calcite within the sandstone (Table 3). This may be partly a problem caused by limited sample size, constrained by the availability of core material from oilfield boreholes. While the quantity of sample required for analysis is small (approximately 1 g), using a sub-sample from a much larger sample (assuming effective homogenisation) might have reduced the discrepancy by incorporating more crystals of calcite in the experimental procedures.

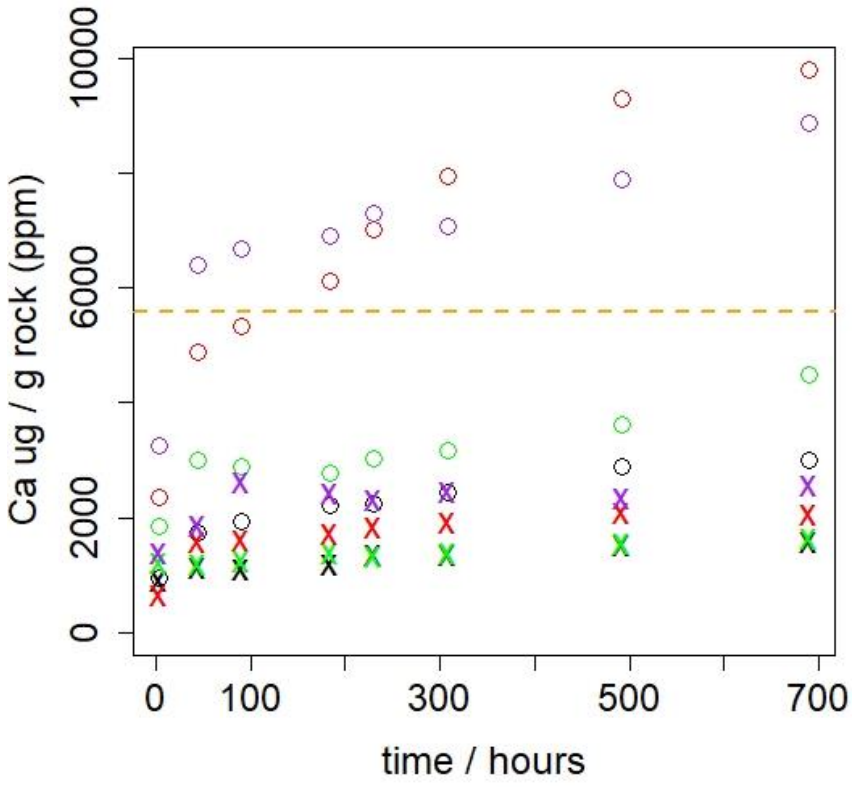

Fig. 5 – Calculated mass of calcium released during the leaching experiments. Note the reaction appears to be ongoing for at least 2 of the flasks at the end of the experiments (red and purple circles: sample SA10 with CO_2). The orange dotted line is the whole-rock total Ca for sample SA7.

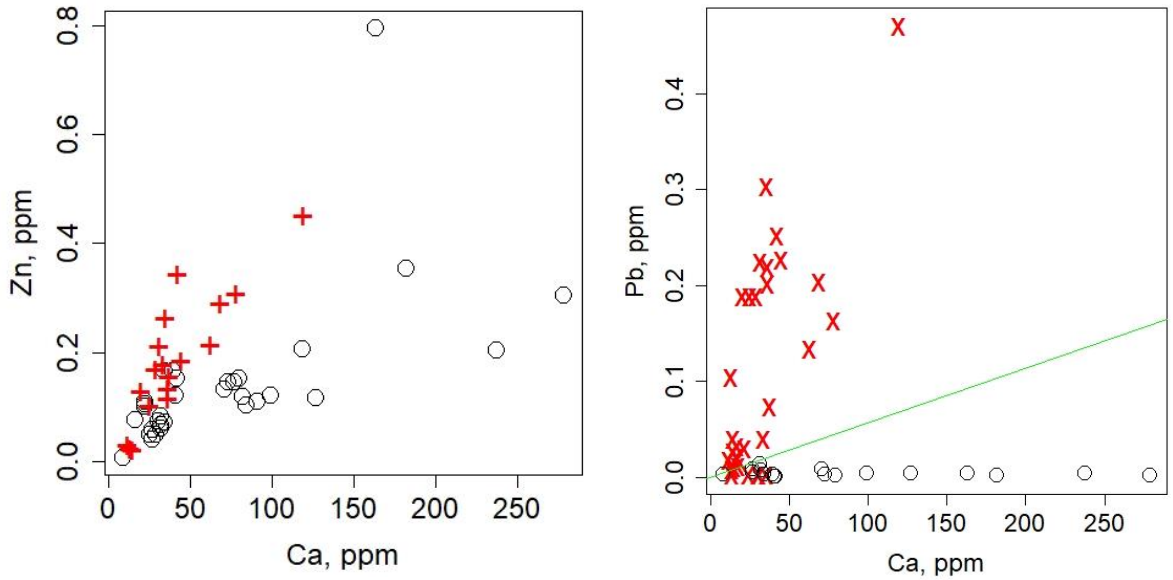

Fig 6A (left). Zn versus Ca in the leaching experiments show different ratios for samples SA7 (red crosses) and SA10 (black circles), for both $+CO_2$ and $-CO_2$ flasks (not differentiated).

Fig. 6B (right) - Pb versus Ca shows 2 trends, neither lies close to the ratio of Pb : Ca from the carbonate stage of the selective extraction procedure (green line).

Of the elements mobilised by the CO_2, Zn correlates weakly overall with Ca (Fig. 6A), however rock samples SA7 and SA10 form separate trends. Zn could hence be interpreted to be released by the dissolution of calcite with differing Zn contents in the 2 samples, higher for SA7. However, the carbonate phase of the selective extraction procedure did not liberate Zn in detectable quantities, and the quantity of Zn leached is a very high proportion of that present in the whole rock (c. 25 – 80 %; Table 5). Hence, if the Zn were derived by the dissolution of calcite, then almost all of the calcite would have to be dissolved. The calculated dissolved mass of Ca however, ranges from c. 1 – 10 μg / g rock, a small proportion of the c. 2900 ppm determined in the carbonate stage of the selective extraction procedure (Table 6). An alternative explanation of the correlation of Zn with Ca is that it reflects a common control, possibly pH change or time for slow desorption and dissolution reactions. Given that the mean mass of Zn leached per g of rock is close to the total in the bulk rock analysis, the preferred explanation is that the Zn is present in the sandstones absorbed onto mineral (Fe, Mn and Al oxides or hydroxides, clay minerals; Lions et al., 2014) or organic surfaces, and is hence released almost entirely during the leaching experiments.

The same patterns and arguments apply to Pb (Fig. 6B) which for sample SA7 would require in excess 10 % of the total calcite to be dissolved if it were to be obtained from this source, i.e. far in excess of the quantity dissolved as inferred from the measured Ca concentrations. As an alternative source, Pb is typically present in K-feldspars in the range of 10 – 1000 ppm (Smith and Brown, 1988), though for sample SA7 the Pb concentrations (relative to K) would require dissolution of a feldspar with > 1 % Pb, which is unfeasible, or for much of the liberated K to be precipitated as, for example, a K-rich clay mineral such as illite. For SA10, which has much lower concentrations of Pb compared to K (median 30 and 70000 μg/L with CO_2, respectively), there is no correlation between the two elements. This either indicates that the dissolution of K-feldspar is not the source of the Pb, or that the individual feldspar crystals have varying Pb contents and reactivities. Interestingly, modelling using Phreeqc indicates an equilibrium K concentration of c. 30,000 μg / L in the presence of K-feldspar and quartz under the experimental conditions, which is the upper boundary of observed K concentrations, possibly implying an approach to equilibrium with K-feldspar for sample SA10. It is hence difficult to quantify the contribution of K-feldspar dissolution to the Pb budget for sample SA10, though a contribution certainly cannot be excluded. The contribution of plagioclase dissolution is even more difficult to quantify, as all the major elements contributed by plagioclase are also sourced from carbonates (Ca), other alumino-silicates (Si, Al) or dissolved in porewater in concentrations that substantially exceed any likely contribution from plagioclase (Na). Hence, from the above discussion, Pb is also interpreted to be desorbed from mineral (clay minerals; Fe-oxides) and / or organic matter surfaces with the possible exception of the Pb in sample SA10 which could be sourced from K-feldspars. Given that both Pb and Zn are sourced by desorption, this would make for difficult prediction of likely mobilisation during CO_2 injection, as the measurement of absorbed Pb and Zn on mineral surfaces will not be simple. Neither the selective extraction procedure nor the whole rock analysis appears to provide useful information in this context and are not viable alternatives to the leaching experiments. Indeed, the simplest method for the determination of trace metal will most likely be desorption under simulated reservoir conditions, as with the leaching experiments reported here.

Lions et al. (2014) noted that, for both Pb and Zn, dissolution experiments conducted in a laboratory setting (e.g. Little and Jackson, 2010; Lu et al., 2010) show significantly higher degrees of mobilisation than in-situ experiments (Kharaka et al., 2010; Trautz et al., 2013; Cahill and Jakobsen, 2013). It has hence been suggested that, in natural systems, scavenging of mobilised metals along fluid flow paths reduces Pb and Zn concentrations, which are artificially intensified under laboratory conditions (Lions et al., 2014). It is therefore concluded that the relatively high Pb and Zn concentrations in the experiments reported here are unlikely to be found in a subsurface injection scenario. Hence, if porewater from the Captain Sandstone Member were to be produced to the surface and disposed of by over-boarding into the North Sea, then the trace element load of the waters will be comparable to existing practise during hydrocarbon operations, and experimental tests such as those presented here would represent overestimates of the potential for metal pollution.

4.2 Limitations of the experimental method

Because the rock samples utilised in the experiments reported here are from oilfield core, they have been potentially contaminated by the 'mud' used in drilling, an issue that has long been known to make difficult the extraction of uncontaminated porewaters from core samples e.g. Lovelock et al. (1975). Such mud contains barite (North, 1985) and for borehole 13/24a-4 had KCl contents of c. 60 mg / L at the relevant depth of drilling (unpublished End of Well Report by Haliburton for BG Exploration and Production, 1998). There is a correlation between K and Ba for sample SA10 which is significant for 95 % confidence (Fig. 7; $R^2 = 0.35$, n = 32) but not for SA7 ($R^2 = 0.01$, n = 28). The range of concentrations for the 2 samples used is similar for Ba, but significantly different for K (Fig. 7). Modelling a solution in equilibrium with barite using Phreeqc gives a concentration of c. 2400 μg / L under the conditions of the experiments. As many of the Ba concentrations exceed the modelled value, and there is no clustering around the value, it is concluded that barite is not buffering Ba, nor even an significant source of the element in the experiments. For K, simple mass balance shows that the experimental concentrations massively exceed those that could be produced even if the porefluids within the sandstone were fully replaced by drilling mud, and this were evaporated to dryness during sample storage, and then fully re-dissolved in the experimental brine (calculated at c. 50 μg / L). Phreeqc modelling indicates an equilibrium concentration of K of c. 30,000 μg / L in the presence of K-feldspar and quartz, which is the upper boundary of observed concentrations, possibly implying an approach to equilibrium during the experiments for sample SA10. Sample SA7 has much lower concentrations, so that either K-feldpar is absent (and the K comes from another source), or any present is less reactive due to for example, a much lower surface area. Either way, there is no evidence to support significant contamination of the samples by drilling mud.

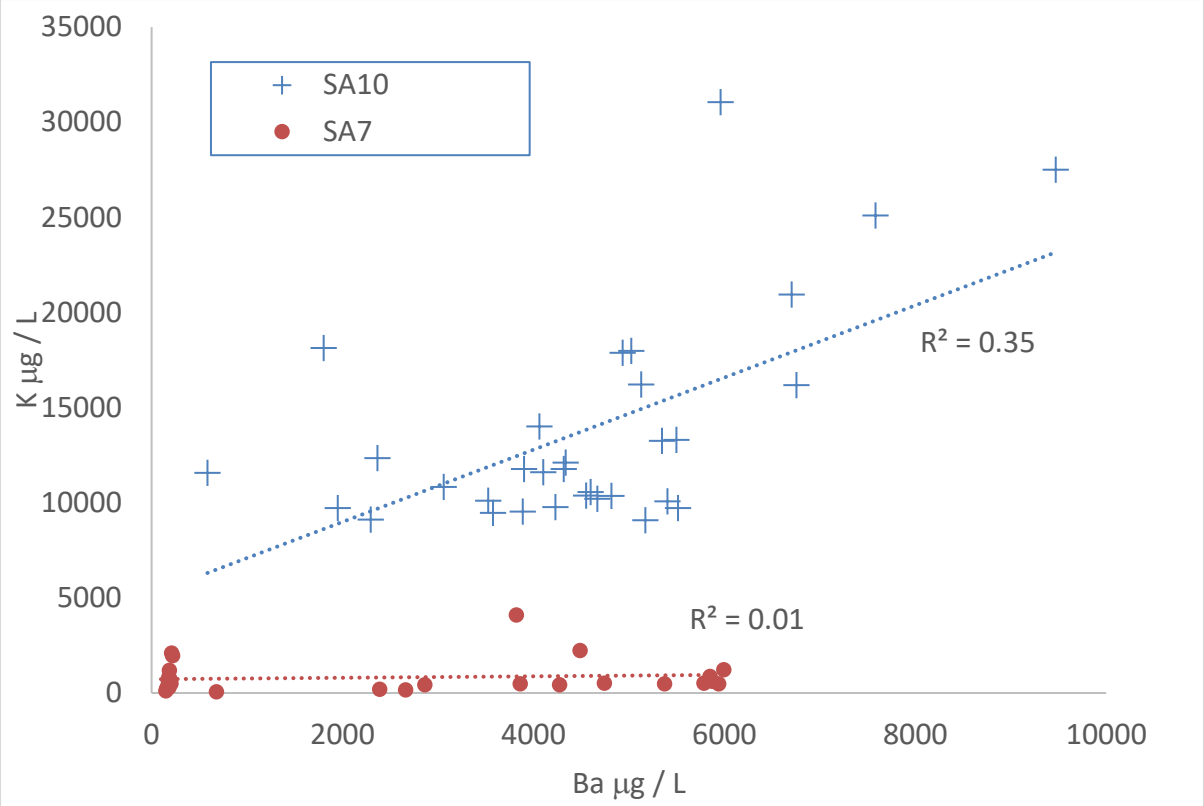

Fig. 7 – Possible indicators of rock sample contamination by drilling mud. There is no strong relationship between K and Ba. The range of concentrations for the 2 samples (SA7 in red, SA10 in black) is similar for Ba, but significantly different for K.

The experiments here were conducted in open flasks, which though flushed with CO_2 were in contact with the atmosphere through the condenser, as were the reagents prior to the start of the experiments. The redox conditions will hence differ from those likely to be found in the subsurface, although the oxygen partial pressure was most likely substantially below that of the atmosphere for much of the duration of the experiments. The duration of the experiments was very short compared to the hoped-for residence time of CO_2 in engineered storage (10,000 years) or even the lifetime of a typical CO_2 injection facility (30 – 50 years?). Longer experiments are logistically more difficult. However, calculated trace metal loads are either stable or falling by the end of the experiments (Fig. 3), so there is no evidence that running the experiments for longer would materially alter the conclusions of the work.

In the experiments reported here, the initial porewater were not in equilibrium with the mineral phases in the rock samples. Hence, some initial reaction between brine and host rock would be expected; this would not be due to the presence of the CO_2. Here, control experiments were ran without added CO_2, so that any reactions due to this disequilibrium will be common to both control and CO_2 flasks. For this reason, the leaching of Cu is interpreted to be due to the establishment of initial equilibrium, as concentrations are similar for control and CO_2 flasks (median 90 µg/L without CO_2; 100 µg/L with CO_2), despite both being higher than the EEMS data (median 0.8 µg/L). Other authors have run parallel experiments with an inert gas (N_2) as a control (e.g. Weibel et al., 2014) or

attempted to recreate the chemistry of the in-situ brine as closely as practicable (e.g. Fisher et al., 2010). An alternative approach, to leave the experiments to reach equilibrium before adding the CO_2, has not been attempted most likely due to the excessive time required, or the difficulty of establishing that equilibrium has been established.

All of the experiments reported in the literature, including those reported here, are run under conditions in which bacteria or other micro-organisms can survive. There is no evidence of biological activity in the experiments, but neither is there proof that such activity did not take place. The role of micro-organisms in subsurface reactions has long been recognised, most commonly in mudrocks (e.g. Irwin et al., 1977) and more controversially in sandstones (e.g. Folk and Lynch, 1997). The possibility of interference of micro-organisms in the experiments cannot hence be eliminated. A biocide could possibly have been added to the experiments to prevent this.

The results from the two rock samples used (SA7 and SA10) are significantly different for Cu (40 vs 150 μg/L respectively) and Pb (200 μg/L vs BDL), as well as for the total Ca dissolved in the +CO_2 experiments (35000 vs 85000 μg/L; Fig. 6). The results of the leaching experiments therefore agree with the XRD analysis: sample SA10 has more calcite (1.6 ± 0.4 % XRD) than sample SA7 (0.37 ± 0.06, XRD). Given that calcite is typically present in deeply buried sandstones as unevenly distributed single crystals, this is not surprising. As the differences are not due to sample contamination by drilling mud, they demonstrate natural sample heterogeneity, a feature of sandstones. Consequently, a leaching experiment based upon a single rock sample, even if replicated, cannot capture natural variation within a reservoir. To fully characterise the likely trace metal load of any produced waters would require a representative number of rock samples, presumably spread throughout the reservoir of interest, to capture the inevitable natural heterogeneity.

The analytical limit of detection (LoD) for 7 of the 8 trace metals is less than the predicted no-effect concentrations (PNEC; Table 2). The exception is Cu, where the LoD (2.9 μg / L) exceeds the PNEC value (2.6 μg / L). As the two values differ by only c. 10%, this is not considered to influence the conclusions of this study. It is also noted that the concentrations of Cu in both the CO_2 and no-CO_2 experiments (median 100 μg/L with CO_2; 90 μg/L without CO_2) substantially exceed the LoD and PNEC values (2.9 and 2.6 μg / L respectively; Table 2), and that although the experimental Cu concentrations substantially exceed that of the Captain Sandstone data from the EEMS database (median 0.8 μg/L), there is no evidence that the CO_2 enhances the leaching.

5. Conclusions

Batch experiments using samples of the Captain Sandstone Member suggest that the mobility of 8 potentially toxic trace metals is low in the presence of high concentrations of CO_2. The concentrations of these metals leached from sandstones are often lower than analytical detection limits, which are (for 7 of the 8 trace metals considered) lower than concentrations recommended by the OSPAR commission for produced water discharges from offshore installations. Where analysis

was possible, the concentrations generally are similar to those of natural brine from the Captain Sandstone Member, suggesting minimal extra trace metal load compared to existing hydrocarbon operations.

For As, Cd, Cr, Hg, and Pb, the experiments have effectively recreated trace metal load of the native porewaters of the Captain Sandstone aquifer despite the difference in pressure, redox and timescale of the experiments compared to in-situ subsurface conditions. The use of rock chips versus disaggregated grains made little difference to the results, the only elements that show any apparent difference are those for which the majority of analyses were below the limit of detection (As, Cd) so that a meaningful interpretation cannot be made. Arsenic concentrations notably decreased in the presence of CO_2, probably due to increased absorption onto Fe-oxides under lowered pH conditions.

Only Pb and Zn were convincingly mobilised during the CO_2 – rich experiments mobilised (median 30 vs 2 μg/L for Pb; 130 vs 25 μg/L for Zn), and are interpreted to have been desorbed from mineral or organic matter surfaces, although the contribution from the dissolution of feldspars is difficult to quantify. Both Pb and Zn have been previously reported to be more easily mobilised in experiments than during in-situ CO_2 injection, due to re-absorption onto mineral surfaces. It is hence considered that the production of native porewater from the Captain Sandstone Member, for pressure control during the injection of CO_2, is unlikely to produce a higher load of trace metals than existing oil and gas production from the same reservoir.

The results from the two rock samples used are significantly different for Cu (median 40 vs 150 μg/L) and Pb (median 200 μg/L vs BDL), although they are from the same reservoir sandstone. Consequently, a representative number of samples would have to be used to determine potential reaction with a high degree of confidence.

Neither the whole-rock analysis nor the selective extraction procedure (either of which could have provided quicker and cheaper alternatives to the leaching experiment) provided useful information about the leached trace metal loads. Consequently, the leaching experiments appear to be the only practical way to assess trace metal loading.

Acknowledgements

KC was co-funded by the UK EPSRC and ScottishPower. Neither organisation was involved in the design or interpretation of the work. We thank Walter Geibert for assisting in the ICP-OES analysis. We thank the British Geological Survey for the core samples. Two reviewers contributed to the clarity and accuracy of the manuscript.

References:

Allen, M.J., Faulkner, D.R., Worden, R.H., Rice-Birchall, E., Katirtsidis, N., and Utley, J.E.P., 2020. Geomechanical and petrographic assessment of a CO2 storage site: Application to the Acorn CO_2 Storage Site, offshore United Kingdom. International Journal of Greenhouse Gas Control 94, 102923.

Boiteau, R. M., Till, C. P., Ruacho, A., Bundy, R. M., Hawco, N. J., McKenna, A. M., Barbeau, K. A., Bruland, K. W., Saito, M. A., & Repeta, D. J., 2016. Structural Characterization of Natural Nickel and Copper Binding Ligands along the US GEOTRACES Eastern Pacific Zonal Transect. Frontiers in Marine Science 3, 1-16. doi:10.3389/fmars.2016.00243

Bowman, K. L., Hammerschmidt, C. R., Lamborg, C. H., & Swarr, G., 2015. Mercury in the North Atlantic Ocean: The U.S. GEOTRACES zonal and meridional sections. Deep Sea Research Part II: Topical Studies in Oceanography 116, 251–261. doi:10.1016/j.dsr2.2014.07.004

Cahill, A. G. and Jakobsen, R., 2013. Hydro-geochemical impact of CO_2 leakage from geological storage on shallow potable aquifers: A field scale pilot experiment. International Journal of Greenhouse Gas Control 19, 678–688.

Cahill, A. G., Jakobsen, R., Mathiesen, T. B., and Jensen, C. K., 2013. Risks attributable to water quality changes in shallow potable aquifers from geological carbon sequestration leakage into sediments of variable carbonate content. International Journal of Greenhouse Gas Control 19, 117–125.

Cutter, G.A., L.S. Cutter, and A.M. Featherstone, 2001. Antimony and arsenic biogeochemistry in the western Atlantic Ocean. Deep-Sea Research, 48:2895-2915.

Fischer, S., Liebscher, A., and Wandrey, M., 2010. CO_2 –brine–rock interaction — First results of longterm exposure experiments at in situ P–T conditions of the Ketzin CO_2 reservoir. Chemie der Erde - Geochemistry 70, 155–164.

Folk, R.L. (1974) Petrology of sedimentary rocks, 170 pp. Austin. Texas, Hemphill Publication Company.

Folk, R.L., and Lynch, F.L., 1997. The possible role of nannobacteria (dwarf bacteria) in clay-mineral diagenesis and the importance of careful sample preparation in high-magnification SEM study. Journal of Sedimentary Research 67, 583-589.

Hsia, T-H, Lo, S.-L., Lin, C.-F. and Lee, D.-Y., 1994. Characterization of arsenate adsorption on hydrous iron oxide using chemical and physical methods. Colloids and Surfaces A: Physicochemical and Engineering Aspects 85, 1-7.

Irwin, H., Curtis, C., and Coleman, M., 1977. Isotopic evidence for source of diagenetic carbonate formed during burial of organic-rich sediments. Nature,269, 209-213.

Jeandel, C., and Minster, J. F., 1987. Chromium behavior in the ocean: global versus regional processes. Global Biogeochemical Cycles 1, 131-154.

Kirsch, K., Navarre-Sitchler, A. K., Wunsch, A., and McCray, J. E., 2014. Metal release from sandstones under experimentally and numerically simulated CO_2 leakage conditions. Environmental Science & Technology 48, 1436–1442.

584 Kjöller, C., Weibel, R., Bateman, K., Laier, T., Nielsen, L. H., Frykman, P., and Springer, N., 2011.
585 Geochemical impacts of CO2 storage in saline aquifers with various mineralogy - Results from
586 laboratory experiments and reactive geochemical modeling. Energy Procedia 4, 4724–4731.

587 Kharaka, Y. K., Thordsen, J. J., Kakouros, E., Ambats, G., Herkelrath, W. N., Beers, S. R., Birkholzer, J.
588 T., Apps, J., Spycher, N. F., Zheng, L., Trautz, R. C., Rauch, H.W., and Gullickson, K. S., 2010. Changes
589 in the chemistry of shallow groundwater related to the 2008 injection of CO_2 at the ZERT field site,
590 Bozeman, Montana. Environmental Earth Sciences 60, 273–284.

591 Lions, J., Devau, N., De Lary, L., Dupraz, S., Parmentier, M., Gombert, P., and Dictor, M. C., 2014.
592 Potential impacts of leakage from CO_2 geological storage on geochemical processes controlling fresh
593 groundwater quality: a review. International Journal of Greenhouse Gas Control 22, 165–175.

594 Little, M. G.; Jackson, R. B., 2010. Potential impacts of leakage from deep CO_2 geosequestration on
595 overlying freshwater aquifers. Environ. Sci. Technol. 44, 9225 – 9232.

596 Lovelock, P. E. R., Price, M., Tate, T. K., J., 1975. Inst. Water Eng., 29, 157-74.

597 Lu, J., Mickler, P. J., Nicot, J.-P., Yang, C., and Romanak, K. D., 2014. Geochemical impact of oxygen
598 on siliciclastic carbon storage reservoirs. International Journal of Greenhouse Gas Control 21, 214–
599 231.

600 Lu, J., Partin, J. W., Hovorka, S. D., and Wong, C., 2010. Potential risks to freshwater resources as a
601 result of leakage from CO_2 geological storage: a batch-reaction experiment. Environmental Earth
602 Sciences 60, 335–348.

603 Melvin, K., Cummine, C., Youles, J. and Williams, H.L., Graham, G.M. and Dyer, S.J., 2008. Optimising
604 calcium naphthenate control in the Blake Field. Society of Petroleum Engineers 114123.

605 Mickler, P. J., Yang, C., Scanlon, B. R., Reedy, R., and Lu, J., 2013. Potential impacts of CO2 leakage on
606 groundwater chemistry from laboratory batch experiments and field push-pull tests. Environmental
607 Science and Technology 47, 10694–10702.

608 Middag, R., van Heuven, S. M. A. C., Bruland, K. W., & de Baar, H. J. W., 2018. The relationship
609 between cadmium and phosphate in the Atlantic Ocean unravelled. Earth and Planetary Science
610 Letters 492, 79–88. doi:10.1016/J.EPSL.2018.03.046

611 North, F.K., 1985, Petroleum Geology. Allen and Unwin, London.

612 OSPAR Commission (2014). Establishment of a list of Predicted No Effect Concentrations (PNECs) for
613 naturally occurring substances in produced water (OSPAR Agreement 2014-05).
614 https://assets.publishing.service.gov.uk/government/uploads/system/uploads/attachment_data/file
615 /361476/OSPAR_RBA_Predicted_No_Effect_Concentrations__PNECs__Background_Document.pdf
616 Accessed 18.5.2020.

617 Pale Blue Dot Energy, 2016. Progressing Development of the UK's Strategic Carbon Dioxide Storage
618 Resource. https://pale-blu.com/2016/04/25/progressing-development-of-the-uks-strategic-carbon-
619 dioxide-storage-resource/
620

621 Pinnock, S. J., Clitheroe, A. R. J. and Rose, P. T. S., 2003. The Captain Field, Block 13/22a, UK North
622 Sea. In: Geological Society, London, Memoir 20, 431-441.

623 Rosenbauer, R. J., Koksalan, T., and Palandri, J. L., 2005. Experimental investigation of CO_2-brine-rock
624 interactions at elevated temperature and pressure: Implications for CO_2 sequestration in deep-saline
625 aquifers. Fuel Processing Technology 86, 1581–1597.
626
627 SCCS, 2011, Progressing Scotland's CO_2 storage opportunities.
628 http://www.geos.ed.ac.uk/sccs/progress-to-co2-storage-scotland/ProgressingScotlandCO2Opps.pdf

629 Schlitzer, R. and 286 others, 2018. The GEOTRACES Intermediate Data Product 2017. Chemical
630 Geology 493, 210–223. doi:10.1016/j.chemgeo.2018.05.040

631 Shiraki, R. and Dunn, T. L., 2000. Experimental study on water-rock interactions during CO2 flooding
632 in the Tensleep Formation,Wyoming, USA. Applied Geochemistry 15, 265–279.

633 Smith, J.V. and Brown, W.L., 1988. Feldspar Minerals, Volume 1, Crystal structures, physical,
634 chemical and microtextural properties. Springer-Verlag, Berlin.

635 Tessier, A., Campbell, P. G. C., & Bisson, M., 1979. Sequential Extraction Procedure for the Speciation
636 of Particulate Trace Metals. Analytical Chemistry 51:844–851.

637 Trautz, R. C., Pugh, J. D., Varadharajan, C., Zheng, L., Bianchi, M., Nico, P. S., Spycher, N. F., Newell, D.
638 L., Esposito, R. A., Wu, Y., Dafflon, B., Hubbard, S. S., and Birkholzer, J. T., 2013. Effect of Dissolved
639 CO_2 on a Shallow Groundwater System: A Controlled Release Field Experiment. Environmental
640 Science & Technology 47, 298-305.

641 Vandecasteele, C. and Block, C. B., 1993. Modern Methods for Trace Element Determination. John
642 Wiley & Sons Ltd., Chichester.

643 Varadharajan, C., Tinnacher, R. M., Pugh, J. D., Trautz, R. C., Zheng, L., Spycher, N. F., Birkholzer, J. T.,
644 Castillo-Michel, H., Esposito, R., and Nico, P. S., 2013. A laboratory study of the initial effects of
645 dissolved carbon dioxide (CO2) on metal release from shallow sediments. International Journal of
646 Greenhouse Gas Control 19, 183–211.

647 Weibel R., Kjøller, C., Bateman, K., Laier, T., Nielsen, L.H., Purser, G., 2014. Carbonate dissolution in
648 Mesozoic sand- and claystones as a response to CO_2 exposure at 70°C and 20 MPa. Applied
649 Geochemistry 42, 1–15.

650 Wigley, M., Kampman, N., Chapman, H. J., Dubacq, B., & Bickle, M. J., 2013. In situ redeposition of
651 trace metals mobilized by CO_2-charged brines. Geochemistry, Geophysics, Geosystems 14, 1321–
652 1332. http://doi.org/10.1002/ggge.20104

653 Wyatt, N. J., Milne, A., Woodward, E. M. S., Rees, A. P., Browning, T. J., Bouman, H. A., Worsfold, P.
654 J., & Lohan, M. C., 2014. Biogeochemical cycling of dissolved zinc along the GEOTRACES South
655 Atlantic transect GA10 at 40°S. Global Biogeochemical Cycles 28, 44–56. doi:10.1002/2013GB004637

656

657

Zheng, L. and Spycher, N., 2018. Modeling the potential impacts of CO_2 sequestration on shallow groundwater: The fate of trace metals and organic compounds before and after leakage stops. Greenhouse Gas Sci Technol. 8, 161–184. DOI: 10.1002/ghg

662 Table 4A. Porewater composition of the batch experiments with added CO_2 No blank correction except for Hg (blank experiments excepted).

663

Flask	Type	Bubbled CO_2	Date	Days	Hours	pH	HCO_3^- mg/L	CO_3^{2-} mg/L	Al µg/L	As µg/L	Ba µg/L	Ca µg/L	Cd µg/L	Cr µg/L	Cu µg/L	Fe µg/L	Hg µg/L	K µg/L	Mg µg/L	Mn µg/L	Na µg/L	Ni µg/L	Pb µg/L	Ti µg/L	U µg/L	V µg/L	Zn µg/L
F1	Blank	Y	31/05/2011	1	4	4.66	65	30	14.02	0	6.04	1750	0.0046	0	54.37	178.07	2.22	445.13	37.96	1.42	0	0	0	0	0	1.95	5.6
F1	Blank	Y	01/06/2011	2	16	4.30	50	25																			
F1	Blank	Y	02/06/2011	3	45	4.45	25	10	175.81	0	9.63	1640	0.21	0.46	91.51	14.18	5.63	358.02	36.58	1.26	0	0	3.58	0		1.49	0
F1	Blank	Y	03/06/2011	4	69.5	4.77	50	25																			
F1	Blank	Y	04/06/2011	5	91	4.73	30	15	5.02	0	8.34	390	0.43	0	157.77	118.3	3.96	323.34	20.31	2.55	0	15.48	0	0	0	1.52	61.24
F1	Blank	Y	05/06/2011	6	109.5	5.36	65	30																			
F1	Blank	Y	06/06/2011	7	137	4.60	55	25																			
F1	Blank	Y	08/06/2011	9	183.5	4.51	50	25	148.39	1.67	0	1830	0	0	66.01	0	2.34	87.86	0	0	876.49	54.88	0	0	0	0	0
F1	Blank	Y	09/06/2011	10	210.5	4.06																					
F1	Blank	Y	10/06/2011	11	229.5	4.27	45	20	70.95	0	2.47	1140	0	0	103.98	0	2.26	291.72	0	0	756.13	3.09	13.22	0	0	0	0
F1	Blank	Y	12/06/2011	13	285	3.96																					
F1	Blank	Y	13/06/2011	14	308	3.90	55	25	226.03	0	5.09	1630	0	0.18	102.67	34.56	2.22	146.59	23.46	0	1635.37	5.16	2.79	0	0	0	0
F1	Blank	Y	15/06/2011	16	349.5	3.91																					
F1	Blank	Y	21/06/2011	22	491.5	5.01	55	30	5.02	0	0	0	0	0.87	147.9	35.97	1.84	1187.48	83.86	0	4650.49	0	4.06	0	0	0	0
F1	Blank	Y	29/06/2011	30	689.5	4.95	50	25	203.86	0	11.49	1600	0	0.66	83.6	48.76	1.85	1526.74	19.97	1.05	8504.05	0.19	6.26	6.56	0	0	0
F2	SA7_Chip	Y	31/05/2011	1	4	4.79	50	25	0	0	679.81	11030	0.2554	1.3002	12.77	0	0	57.12	151.05	24.83	0	9.9794	104.3051	0	0	0	19.1
F2	SA7_Chip	Y	01/06/2011	2	16	5.03	80	40																			
F2	SA7_Chip	Y	02/06/2011	3	45	6.20	105	50	0	0	2389.41	23370	0.15	0	13.43	433.02	0	189.11	288.19	106.96	0	10.8294	185.3	0	0	0.43	101.73
F2	SA7_Chip	Y	03/06/2011	4	69.5	6.23	105	50																			
F2	SA7_Chip	Y	04/06/2011	5	91	6.11	105	50	14.38	0	2861.94	28350	0	3.4202	7.71	0	0	424.73	387.28	132.72	0	1.23	188.4351	0	0	0.19	108.22
F2	SA7_Chip	Y	05/06/2011	6	109.5	6.46	120	60																			
F2	SA7_Chip	Y	06/06/2011	7	137	6.46	120	60																			
F2	SA7_Chip	Y	08/06/2011	9	183.5	6.12	120	60	0	0	3861.34	34160	0	1.0002	67.55	34.075	0	475.59	617.997	199.5843	0	0	201.6351	0	0	0	115.07
F2	SA7_Chip	Y	09/06/2011	10	210.5	6.10																					
F2	SA7_Chip	Y	10/06/2011	11	229.5	6.40	135	65	0	0	4273.37	35150	0	0.5702	42.25	110.385	0	435.34	649.417	227.3943	0	8.85	206.28	0	0	0	132.09
F2	SA7_Chip	Y	12/06/2011	13	285	5.99																					
F2	SA7_Chip	Y	13/06/2011	14	308	6.12	160	80	0	0	4741.99	43170	0	0.63	33.74	283.88	0	513.76	793.36	281.0443	0	10.09	223.85	0	0	0	184.66
F2	SA7_Chip	Y	15/06/2011	16	349.5	6.18																					
F2	SA7_Chip	Y	21/06/2011	22	491.5	6.99	185	90	0	0	5993.14	68331	0	0	61.61	0	0	1223.8	1410.03	539.5143	0	22.1094	200.14	12.31	0	0	288.29
F2	SA7_Chip	Y	29/06/2011	30	689.5	7.43	235	115	0	0	5849.43	76530	0	0	86.29	263.97	0	870.26	1847.45	683.98	0	24.31	157.04	0	0	0	306.04
F3	SA7_Grain	Y	31/05/2011	1	4	5.19	105	50	0	4.285	2660.24	18410	0.2654	1.5902	26.11	0	0	170.13	179.3	59.41	0	3.4994	189.1651	0	0	0	124.04
F3	SA7_Grain	Y	01/06/2011	2	16	5.65	115	55																			
F3	SA7_Grain	Y	02/06/2011	3	45	6.39	100	50	0	0	5941.05	33450	0	0	82.93	922.62	0	482.87	357.22	187.91	0	3.5694	299.56	0	0	2.36	262.99
F3	SA7_Grain	Y	03/06/2011	4	69.5	6.66	150	75																			
F3	SA7_Grain	Y	04/06/2011	5	91	6.92	95	45	137.92	0	5785.26	32780	0	3.9502	0	0	0	515.51	493.16	136.25	0	0.43	39.5951	0	0	0.35	116.99
F3	SA7_Grain	Y	05/06/2011	6	109.5	7.34	115	55																			
F3	SA7_Grain	Y	06/06/2011	7	137	8.20	115	55																			
F3	SA7_Grain	Y	08/06/2011	9	183.5	6.09	125	60	0	0	5872.78	29480	0	1.5002	145.13	53.025	0	611.66	627.587	185.9843	0	0	225.0951	0	0	0	209.95
F3	SA7_Grain	Y	09/06/2011	10	210.5	5.90																					
F3	SA7_Grain	Y	10/06/2011	11	229.5	6.75	120	60	0	0	5372.93	35890	0	0	34.72	0	0	487.76	639.007	197.9143	0	376.35	60.63	0	0	0	154.04

F3	SA7_Grain	Y	12/06/2011	13	285	5.78																				
F3	SA7_Grain	Y	13/06/2011	14	308	5.99	130	65	0	0	5592.67	40460	0	0.45	151.11	167.71	0	0	823.14	252.4843	0	5.22	248.95	4.18	0	0	342.14
F3	SA7_Grain	Y	15/06/2011	16	349.5	5.93																				
F3	SA7_Grain	Y	21/06/2011	22	491.5	6.95	165	80	0	0	4487.62	62381	0	0	4.47	17.29	0	2231.56	1529.78	476.6843	1611.6	14.2194	129.85	2.2	0	0	211.79
F3	SA7_Grain	Y	29/06/2011	30	689.5	7.73	290	80	0	0	3821.67	117860	0	0.84	136.52	330.68	0	4097.54	3423.55	1039.15	9033.12	39.55	463.96	22.67	0	0	450.26
F4	SA10_Chip	Y	31/05/2011	1	4	5.73	110	55	0	0.445	1800.99	29870	1.5354	0	158.81	34.29	1.91	18137.23	547.11	93.48	920.68	5.2594	14.4051	0	0	0.78	76.39
F4	SA10_Chip	Y	01/06/2011	2	16	7.77	160	80																			
F4	SA10_Chip	Y	02/06/2011	3	45	6.65	275	135	0	0	4064.25	69230	1.08	0.1	135.75	599.86	0	14009.7	761.47	236.6	0	5.7194	5.18	0	0	1.03	130.82
F4	SA10_Chip	Y	03/06/2011	4	69.5	7.93	275	135																			
F4	SA10_Chip	Y	04/06/2011	5	91	7.42	270	130	25.66	0	4316.46	78990	0.65	5.4102	68.26	307.04	0	11769.78	848.93	222.46	0	34.64	2.2751	0	0	0.89	90.23
F4	SA10_Chip	Y	05/06/2011	6	109.5	7.90	310	155																			
F4	SA10_Chip	Y	06/06/2011	7	137	7.88	300	150																			
F4	SA10_Chip	Y	08/06/2011	9	183.5	6.68	320	160	16.85	0	5348.5	97440	0	0.0902	154.92	395.965	0	13261.9	1476.017	360.1943	0	0	4.0151	15.48	0	0.2644	117.68
F4	SA10_Chip	Y	09/06/2011	10	210.5	6.71																					
F4	SA10_Chip	Y	10/06/2011	11	229.5	7.04	420	200	0	1.245	5499.41	125710	0	0.1902	109	421.465	0	13296.72	1723.267	441.5943	0	10.24	0	0	0	0	114.21
F4	SA10_Chip	Y	12/06/2011	13	285	6.71																					
F4	SA10_Chip	Y	13/06/2011	14	308	6.80	500	240	0	0	5961.91	161690	0	2.14	40.09	629.26	0	31065.41	2579.58	616.6243	0	6.84	1.34	0	0	0	792.58
F4	SA10_Chip	Y	15/06/2011	16	349.5	6.87																					
F4	SA10_Chip	Y	21/06/2011	22	491.5	8.00	650	320	0	0	6705.1	237331	0	1.08	44.55	727.6	0	20946.52	4061.42	883.2543	0	15.7394	0	21.59	0	0	202.61
F4	SA10_Chip	Y	29/06/2011	30	689.5	8.37	800	400	0	0	7583.43	277060	0	0	131.42	0	0	25095.26	5675.71	1058.53	0	19.36	0	9.89	0	0	302.98
F5	SA10_Grain	Y	31/05/2011	1	4	6.66	135	65	0	3.725	2295.08	32580	0.3254	0.7002	209.2	61.22	0	9114.31	349.23	97.97	0	2.9994	2.7951	0	0	1.11	65.35
F5	SA10_Grain	Y	01/06/2011	2	16	7.52	210	105																			
F5	SA10_Grain	Y	02/06/2011	3	45	6.90	270	135	0	0	4668.09	71110	0.14	0.41	239.17	796.42	0	10211.22	674.56	205.19	0	5.1794	0	0	0	1.29	142.45
F5	SA10_Grain	Y	03/06/2011	4	69.5	8.11	260	130																			
F5	SA10_Grain	Y	04/06/2011	5	91	8.01	285	140	15.24	0	4818.3	76480	0	4.1702	138.85	517.5	4.12	10360.14	770.6	148.72	0	0	0	0	0	1.49	84.4
F5	SA10_Grain	Y	05/06/2011	6	109.5	8.29	290	140																			
F5	SA10_Grain	Y	06/06/2011	7	137	8.46	270	135																			
F5	SA10_Grain	Y	08/06/2011	9	183.5	6.59	300	150	0	0	5403.58	79890	0	1.0302	254.27	281.725	0	10077.46	1277.327	286.7543	0	0	0	6.94	0	0	115.48
F5	SA10_Grain	Y	09/06/2011	10	210.5	6.54																					
F5	SA10_Grain	Y	10/06/2011	11	229.5	7.20	335	165	0	0	5515.73	89840	0	1.4702	309.94	488.175	0	9716.52	1473.977	324.7043	0	8.15	0	36.83	0	0	108.56
F5	SA10_Grain	Y	12/06/2011	13	285	6.51																					
F5	SA10_Grain	Y	13/06/2011	14	308	6.52	325	160	0	0	5172.43	82300	0	0	245.56	211.87	0	9072.17	1559.78	404.2643	0	5.11	0	0	0	0	101.63
F5	SA10_Grain	Y	15/06/2011	16	349.5	6.65																					
F5	SA10_Grain	Y	21/06/2011	22	491.5	7.80	370	180	0	0	6754.06	118661	0	0	187.68	0	0	16181.08	3133.22	727.1943	167.28	42.1294	0	1.96	0	0	204.85
F5	SA10_Grain	Y	29/06/2011	30	689.5	8.25	500	240	0	0	9470.43	180290	0	0	467.61	0	0.53	27502.46	5583.91	1139.92	2792.76	20.03	0	11.28	0	0	351.32

668 Table 4B. Porewater composition from the batch experiments with no added CO_2 No blank correction except for Hg (blank experiments excepted)..

Flask	Type	Bubbled CO_2	Date	Days	Hours	pH	HCO_3^- mg/L	CO_3^{2-} mg/L	Al µg/L	As µg/L	Ba µg/L	Ca µg/L	Cd µg/L	Cr µg/L	Cu µg/L	Fe µg/L	Hg µg/L	K µg/L	Mg µg/L	Mn µg/L	Na µg/L	Ni µg/L	Pb µg/L	Ti µg/L	U µg/L	V µg/L	Zn µg/L
B1	Blank	N	31/05/2011	1	4	6.41	55	30	49.41	2.01	11.42	2990	0.71	4.23	55.18	68.63	46858.8	1007.96	224.81	11.55	119.01	0.0406	1.84	10.84	0	1.52	28.7
B1	Blank	N	01/06/2011	2	16	6.67	65	30																			
B1	Blank	N	02/06/2011	3	45	6.57	70	35	0	0	1.79	0	0.16	0.51	76.01	0	13.99	641.17	10.33	1.6	119.01	0.0406	0	0	0	1.36	1.8
B1	Blank	N	03/06/2011	4	69.5	8.26	60	30																			
B1	Blank	N	04/06/2011	5	91	8.26	55	25	0	0	15.18	5270	0	0	93.51	0	6.25	320.69	8.08	0.0657	119.01	0.0406	0	0	0	1.49	7.57
B1	Blank	N	05/06/2011	6	109.5	6.95	55	25																			
B1	Blank	N	06/06/2011	7	137	7.04	20	10																			
B1	Blank	N	08/06/2011	9	183.5	4.77	40	20	196.78	3.97	0	1410	0	0.19	56.9	0	3.89	0	0	0	0	8.52	0	0	0	0	0
B1	Blank	N	09/06/2011	10	210.5	4.66																					
B1	Blank	N	10/06/2011	11	229.5	5.07	50	25	0	0	0	1170	0	2.05	46.98	0	2.72	0	0	0	0	2.12	0	4.55	0	0	0
B1	Blank	N	12/06/2011	13	285	5.35																					
B1	Blank	N	13/06/2011	14	308	5.10	45	20	70.18	0	0	470	0	0	27.17	0	2.97	0	0	0	0	271.12	0	0	0	0	0
B1	Blank	N	15/06/2011	16	349.5	4.80																					
B1	Blank	N	21/06/2011	22	491.5	4.76	55	25	0	0	0	250	0	0	117.4	4.38	4.89	702.17	1.143	0	2122.93	0	1.2	5.45	0	0	0
B1	Blank	N	29/06/2011	30	689.5	5.85	55	30	76.6	0	3.34	1180	0	2.38	78.64	14.67	3.19	892.91	83.23	1.7	2881.81	0	1.77	2.38	0	0	0
B2	SA7_Chip	N	31/05/2011	1	4	6.31	50	25	0	0	97.54	8660	0	0	43.9	60.71	0	0	0	7.07	0	0	16.16	0	0	0.14	2.53
B2	SA7_Chip	N	01/06/2011	2	16	6.91	35	15																			
B2	SA7_Chip	N	02/06/2011	3	45	6.68	45	20	0	0	155.76	14771	0	0.62	0	8.205	0	0	198.36	14.12	0	0	10.5951	0	0	0.76	0
B2	SA7_Chip	N	03/06/2011	4	69.5	7.45	45	20																			
B2	SA7_Chip	N	04/06/2011	5	91	7.37	75	40	0	0	149.94	9100	0.2654	1.6402	14.92	0	0	104.45	196.53	21.0643	0	0	26.4951	0	0	0.1	13.65
B2	SA7_Chip	N	05/06/2011	6	109.5	6.83	55	25																			
B2	SA7_Chip	N	06/06/2011	7	137	6.88	75	35																			
B2	SA7_Chip	N	08/06/2011	9	183.5	5.17	80	40	0	0	180.04	14980	0	0	15.79	0	0	374.4	463.367	28.2543	0	10.41	20.82	0	0	0	0
B2	SA7_Chip	N	09/06/2011	10	210.5	5.34																					
B2	SA7_Chip	N	10/06/2011	11	229.5	6.41	60	30	160.49	0	184.02	20310	0	0	48.84	0	0	301.16	340.967	31.0043	0	2.6	29.8451	0	0	0	0
B2	SA7_Chip	N	12/06/2011	13	285	6.52																					
B2	SA7_Chip	N	13/06/2011	14	308	6.51	70	35	0	0	176.9	20710	0	0	69.77	0	0	608.38	348.517	34.2043	0	0	#REF!	4.22	0	0	0
B2	SA7_Chip	N	15/06/2011	16	349.5	6.53																					
B2	SA7_Chip	N	21/06/2011	22	491.5	6.54	75	35	12.42	0	191.14	30660	0	2.03	0	12.55	0	753.37	686.747	52.8943	361.08	20.8494	1.49	0	0	0	0
B2	SA7_Chip	N	29/06/2011	30	689.5	6.50	75	35	99.55	0	185.83	34050	0	0	47.13	36.35	0	1194.01	780.71	73.27	826.2	2.6194	1.63	0	0	1.8044	0
B3	SA7_Grain	N	31/05/2011	1	4	6.37	60	30	0	0	136.89	10420	0	0	3.43	0	0	0	0	0.28	0	0	6.5	0	0	0	0
B3	SA7_Grain	N	01/06/2011	2	16	7.30	65	30																			
B3	SA7_Grain	N	02/06/2011	3	45	6.73	45	20	0	0.685	180.48	13051	0.09	0.2	11.47	0	4.99	821.31	170.31	19.94	0	0	3.0451	0	0	0.58	0
B3	SA7_Grain	N	03/06/2011	4	69.5	7.02	70	35																			
B3	SA7_Grain	N	04/06/2011	5	91	7.07	65	30	0	2.395	158.16	8900	0.2554	0	21.71	0	0	262.95	170.56	26.7443	0	0	40.0251	0	0	0.27	0
B3	SA7_Grain	N	05/06/2011	6	109.5	6.84	65	30																			
B3	SA7_Grain	N	06/06/2011	7	137	6.79	60	30																			
B3	SA7_Grain	N	08/06/2011	9	183.5	5.23	65	30	0	1.77	201.58	15310	0	1	37.88	0	0	491.7	260.997	33.3943	0	0.54	31.71	10.25	0	0	0
B3	SA7_Grain	N	09/06/2011	10	210.5	5.91																					
B3	SA7_Grain	N	10/06/2011	11	229.5	6.42	75	35	0	3.905	186.08	14240	0	0	43.05	0	0	563.71	260.587	31.4143	0	7.98	#REF!	0	0	0	0
B3	SA7_Grain	N	12/06/2011	13	285	6.46																					
B3	SA7_Grain	N	13/06/2011	14	308	6.54	65	35	0	2.975	189.54	16930	0	1.2702	81.64	0	0	482.72	259.157	35.2243	0	0	11.8951	0	0	0	0

B3	SA7_Grain	N	15/06/2011	16	349.5	6.60																				
B3	SA7_Grain	N	21/06/2011	22	491.5	7.01	95	45	0		218.72	24010	0	1.21	0	0	0	1960.03	509.877	48.4443	1399.44	2.1694	2.35	5.65	0	1.8644	0
B3	SA7_Grain	N	29/06/2011	30	689.5	6.92	80	40	39.54		208.82	28600	0	1.27	9.39	6.28	0	2089.57	728.89	62.68	1717.68	3.3594	1.1	3.74	0	5.4344	145.67
B4	SA10_Chip	N	31/05/2011	1	4	6.84	80	40	0	1.56	585.08	5300	0	0	92.07	0	0	11570.68	62.63	4.19	0	0.6594	1.64	0	0	0.81	#REF!
B4	SA10_Chip	N	01/06/2011	2	16	7.93	75	40																			
B4	SA10_Chip	N	02/06/2011	3	45	7.38	90	45	0	8.035	2364.61	22091	0	0	183.89	0	1.49	12345.47	352.47	67.21	0	0	0	26.01	0	4	106.36
B4	SA10_Chip	N	03/06/2011	4	69.5	7.59	85	45																			
B4	SA10_Chip	N	04/06/2011	5	91	7.96	75	35	0	4.335	3059.1	17150	0	0	206.37	0	0	10823.83	568.12	45.7543	0	0	0	0	0	3.03	96.39
B4	SA10_Chip	N	05/06/2011	6	109.5	8.05	85	40																			
B4	SA10_Chip	N	06/06/2011	7	137	7.97	120	60																			
B4	SA10_Chip	N	08/06/2011	9	183.5	7.12	115	55	0	5.5	3902.14	23680	0	2.22	175.25	0	0	11771.06	809.347	13.4143	0	4.21	0	0	0	2.0444	46.83
B4	SA10_Chip	N	09/06/2011	10	210.5	7.05																					
B4	SA10_Chip	N	10/06/2011	11	229.5	7.31	140	70	125.91		4104.1	27290	0	0	205.37	0	0.67	11597.66	910.537	14.8143	0	559.08	0	0	0	2.5344	47.85
B4	SA10_Chip	N	12/06/2011	13	285	7.49																					
B4	SA10_Chip	N	13/06/2011	14	308	7.37	125	60	12.32	4.475	4338.7	31290	0	0.8302	276.59	0	0.49	12103.58	1021.717	12.6843	0	134.02	7.1751	0.9	0	3.8444	57.65
B4	SA10_Chip	N	15/06/2011	16	349.5	7.55																					
B4	SA10_Chip	N	21/06/2011	22	491.5	7.61	145	70	40.53		5026.18	40550	0	0	267.34	1.69	0	17974.03	1767.537	13.3543	1383.12	3.4494	0	0	0	10.2544	119.21
B4	SA10_Chip	N	29/06/2011	30	689.5	7.37	150	75	15.55		4935.5	37820	0	1.16	250.62	38.37	1.34	17879.17	1767.25	17.21	1122	2.7894	1.4	3.29	0	15.6044	163.52
B5	SA10_Grain	N	31/05/2011	1	4	8.51	80	40	0	8.79	1951.47	12810	0	0	302.02	116.17	0	9724.48	33.39	3.69	0	0	0	0	0	3.71	47.19
B5	SA10_Grain	N	01/06/2011	2	16	8.35	80	40																			
B5	SA10_Grain	N	02/06/2011	3	45	8.30	95	45	77.17	7.675	3576.37	22131	0	0.4	284.66	37.925	0	9473.15	432.96	8.56	0	1.8994	0	0	0	3.63	99.04
B5	SA10_Grain	N	03/06/2011	4	69.5	8.18	125	60																			
B5	SA10_Grain	N	04/06/2011	5	91	8.26	115	55	0	8.915	3889.38	28720	0	0	307.96	0	0.04	9542.71	452.92	9.8443	0	1.2094	0	0	0	5.6	157.69
B5	SA10_Grain	N	05/06/2011	6	109.5	8.33	125	60																			
B5	SA10_Grain	N	06/06/2011	7	137	8.36	135	65																			
B5	SA10_Grain	N	08/06/2011	9	183.5	7.60	130	65	0	5.6	4552.9	28720	0	0.97	308.46	0	1.92	10381.82	817.717	9.2743	0	10.68	0	14.56	0	5.1344	72.15
B5	SA10_Grain	N	09/06/2011	10	210.5	7.35																					
B5	SA10_Grain	N	10/06/2011	11	229.5	7.54	125	60	97.35	2.575	4230.58	25680	0	0	283.3	0	2.8	9773.9	770.387	7.6843	0	5.36	8.6851	0	0	3.7544	56.34
B5	SA10_Grain	N	12/06/2011	13	285	7.70																					
B5	SA10_Grain	N	13/06/2011	14	308	7.60	145	70	79.29	3.665	4599.82	31290	0	0	355.74	0	3.66	10569.5	848.107	6.4243	0	480.42	#REF!	27.85	0	4.5344	65.79
B5	SA10_Grain	N	15/06/2011	16	349.5	7.60																					
B5	SA10_Grain	N	21/06/2011	22	491.5	7.74	155	75	0		3524.74	26230	0	0	180.64	7.07	2.12	10109.83	1012.737	3.3643	0	0	4.32	0	0	6.8944	37.04
B5	SA10_Grain	N	29/06/2011	30	689.5	7.44	165	80	74.24		5129.3	40270	0	0	265.3	26.42	6.57	16218.61	1664.44	11.61	1815.6	1.4394	0	0	0	12.7144	149.02